Available online at www.sciencedirect.com
SCIENCE DIRECT®
PERGAMON
International Journal of Heat and Mass Transfer 46 (2003) 4489–4497
International Journal of HEAT and MASS TRANSFER
www.elsevier.com/locate/ijhmt

The structure of plumes generated in the unidirectional solidification process for a binary system

T. Nishimura *, J. Sasaki, T.T. Htoo

Department of Mechanical Engineering, Yamaguchi University, Ube 755-8611, Japan

Received 21 October 2002; received in revised form 3 March 2003

Abstract

The present article describes the structure of plumes generated during solidification of a binary system. A transparent aqueous ammonium chloride solution is employed for super-eutectic growth in a Hele–Shaw cell. The velocities of plume convection in the melt layer and interstitial fluid flow within the mushy layer are measured by the particle tracking and dye tracing methods, respectively. Several important features are identified for each convective flow. In particular, the plume convection is found to consist of the upward flow enveloped in the downward flow, i.e., double flow structure. The downward flow enhances the solidification in the neighborhood of the exit of the channel emanating the plume, like a volcano. Interstitial fluid within the mushy layer is observed to move downward uniformly, which is induced by the plume convection.
© 2003 Elsevier Ltd. All rights reserved.

1. Introduction

Natural convection flows have been known for some time to have an important influence on solidification processes involving multi-component substances. In recent years, experimental and numerical treatments of solidification in binary systems have been stimulated by engineering applications such as semiconductor crystal growth and the casting of metals. In particular, double-diffusive convection phenomena such as layer formation and merging have received much attention in the melt layer [1–5]. However, the convection within the mushy layer consisting of crystals and interstitial melt has not been understood fully yet [4,9].

In the unidirectional solidification process cooled from below, several channels are formed in localized regions of the mushy layer, known as freckles. The origin of freckles is related to the onset of convection in the mushy layer and therefore experimental studies of channel formation have been focused on the solidification of a transparent NH_4Cl–H_2O system. Recent observations by Chen and Chen [6] and Tait and Jaupart [8] revealed that plume convection and channel formation result from instabilities of the mushy layer. Quantitative measurement of mushy layer properties during channel formation is difficult because the forest of dendritic crystals makes the region opaque. Despite this obstacle, Chen [7] obtained time history of the solid fraction in a growing mushy layer using X-ray tomography. Nishimura et al. [11,12] measured the concentration profile within the mushy layer using a liquid extraction method and estimated the average solid fraction from mass balance. The solid fraction is small, typically around 10% or less, which is close to the result of Chen. Thus, the mushy layer is very permeable and natural convection is likely to occur. Furthermore, they confirmed that the liquid in the mushy layer is in thermodynamic equilibrium except near the mush–melt interface. Solomon and Hartley [10] visualized the temperature field in a growing mushy layer using thermochromic liquid crystal paints, and the bumps in isotherms indicate the onset, growth and decay of convection.

However, there have been no velocity measurements in the mushy layer and melt layer. Such measurements are required for detailed comparison with numerical

* Corresponding author. Tel.: +81-836-85-9121; fax: +81-836-85-9101.
E-mail address: tnishimu@yamaguchi-u.ac.jp (T. Nishimura).

0017-9310/$ - see front matter © 2003 Elsevier Ltd. All rights reserved.
doi:10.1016/S0017-9310(03)00276-X

Nomenclature

D	diameter of channel	t	time
H	height of cell	u_{max}	maximum velocity of plume
h	depth of channel	v	downward velocity of interstitial fluid within the mushy layer
L	length of cell	W	horizontal width of cell
r	radial coordinate of channel		
u	vertical velocity of plume		

simulation and refinement of the solidification model. This motivates the present investigation. In this paper, we present velocity measurements in plumes generated during solidification of a NH_4Cl–H_2O system cooled from below, using several flow visualization techniques. The experiments are complemented by two-dimensional studies in a Hele–Shaw cell, which allows direct visualization of the growth of channels within the mushy layer and simultaneously measurements of the velocity field.

2. Experimental apparatus and procedure

Fig. 1 shows a schematic diagram of the experimental apparatus. Solidification of an aqueous ammonium chloride solution for super-eutectic growth was performed in a Hele–Shaw cell with inner dimensions of 100 mm in height, 50 mm in length and 3 mm in width. A cooling chamber was attached to the bottom of the cell, and the bottom temperature was maintained by refrigeration unit 1. Refrigeration unit 2 was used to control the initial temperature of the aqueous solution. The experimental apparatus was placed in a temperature-controlled room at 25 °C. A solution of 27 wt.% NH_4Cl–H_2O at $T_i = 25$ °C was directionally solidified by maintaining the bottom at $T_c = -14.3$ °C.

Velocity measurements for liquid flows have often performed by laser-Doppler-velocimetry (LDV). However, LDV techniques are difficult to capture time-dependent fine structures such as salt-fingers and plumes generated during solidification due to a point measurement. In the present study, a particle tracking technique is employed to infer the velocity field from video tracking. Magnified images using a microscope provide sufficient spatial resolution. Fig. 2 shows a velocity measurement system employed here. For the flow visualization, seeding with thermochromic liquid crystal particles is used, allowing instantaneous measurement of the velocity to be made. Their diameters range from 10 to 15 μm and the density is close to that of the aqueous solution. It should be noted that if smaller particles of about 1 μm are employed, the particles becomes nucle-

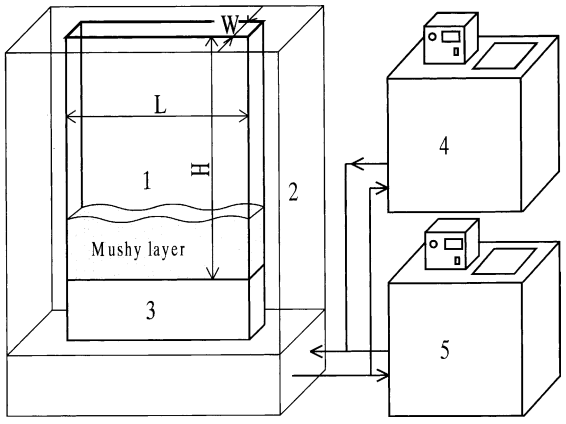

1. Test section (H=100mm, L=50mm, W=3mm)
2. Acrylic wall
3. Cooling chamber
4. Refrigeration unit 1
5. Refrigeration unit 2

Fig. 1. Schematic diagram of experimental apparatus.

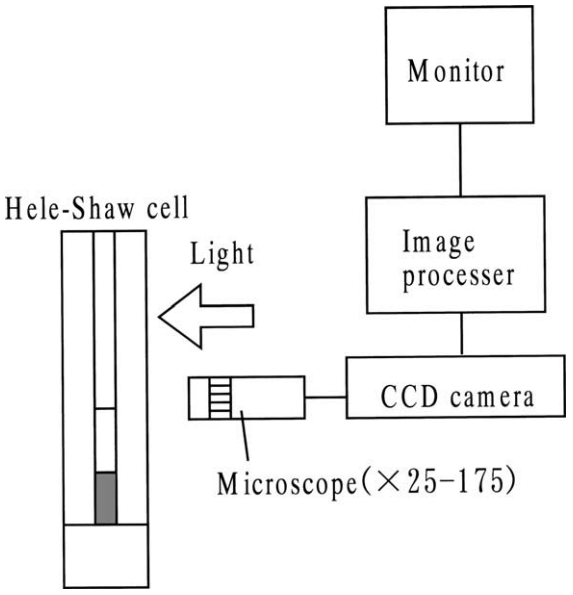

Fig. 2. Schematic diagram of image processing.

ation sites for initiating the growth of equiaxed dendritic crystals in the melt layer. The cell is illuminated with a 3 mm thick sheet of white light from a projector lamp. The images of flow seeding are observed in the perpendicular direction by a CCD-camera with the microscope set up for an adjustable magnification from 25 to 175 times. The 8-bit images of 640×640 pixels resolution are acquired using an image processor. Evaluation of convection is carried out with an interval time of 1/30 s. In addition, another method is used to examine overall flow patterns. The cell is illuminated by three color light sheet at each interval during a long exposure time. So we can determine the starting and terminal points of an aimed particle tracer during the exposure time (so called sequential three color sheet method). Three color lights are made up by white light, passing through red, green and blue sheets in turn. A merit of this method is identification of the flow direction of each particle path.

In the mushy layer, the velocity measurements are very difficult even by using the aforementioned methods. We perform flow visualization using a dye tracing method and simultaneously observe the structure of NH_4Cl crystals. Hele–Shaw cell is more proper to work out this than a three-dimensional tank. Just prior the start of a dye tracing experiment, a small amount of solution is withdrawn from the mush–melt interface and is colored red by Rhodamine B dye. The dye solution is then placed through a capillary tube mounted on a traverse mechanism onto the mush–melt interface. The motion of the dye solution is monitored by a CCD-camera.

A technique using liquid crystal paint enables imaging of a two-dimensional map of the temperature field near the mush–melt interface. A sheet of liquid crystal paint coated is applied to the inside surface of a sidewall of the cell. Despite the fact the fluid is motionless along the side wall, the liquid crystal paint responds the flow in the interior due to the rapid diffusion of heat across the narrow gap, i.e., $W = 3$ mm.

3. Results and discussion

When aqueous ammonium chloride solution with a super-eutectic concentration is directionally solidified from below, a mushy layer is formed below the melt layer due to the undercooling-induced morphological instability. During the solidification process, as a result of the rejection of lighter fluid upon solidification, two different convection patterns are observed.

Fig. 3 shows the growth of the mushy layer. Although the growth is large in the initial stages of solidification, its rate is more retarded with progressing solidification due to the decrease of concentration in the melt layer above the mushy layer. The concentration decrease is due to release of less dense fluid from ammonium chloride crystals. Therefore, an unstably stratified concentration profile is formed including the mushy layer maintained thermodynamic equilibrium, but the temperature profile is stably stratified, which suggests the onset of double-diffusive convection [12]. In this experiment, salt-finger convection and plume convection take place in certain intervals during solidification, and their shadowgraph images are also shown in the figure. The salt-finger convection uniformly starts on the mush–melt interface soon after the experiment, and then it gives way to plume convection. The overlap interval between finger and plume is 50 min.

We briefly describe the differences in the solidification process between the Hele–Shaw cell and a three-dimensional tank, with comparison of the results by Magirl and Incropera [9]. The solidification rate in the Hele–Shaw cell is slightly slower than that of a three-dimensional tank and, no helical plumes are observed because of the suppression of convection in the Hele–Shaw cell. Also the Hele–Shaw cell limits channel formation. However, the qualitative features are identical.

Time history of isotherms near the mush–melt interface and crystal structures of the mushy layer is shown in Fig. 4. The thermochromic liquid crystals paint has a working range of 12.5–14.5 °C, and the green color approximately indicates the 13.5 °C isotherm. Small-wavelength undulations are visible in the isotherms above the mush–melt interface at 5 min 46 s from the start of experiment, indicating fingers. These undulations fade after approximately 10 min, after which only three pronounced bumps are visible, suggesting the onset of plumes. However, one of them finally disappears in this experiment. It should be noted that the crystals at the two bumps grow more rapidly than those at other positions, an indication of channel formation near the interface of the mushy layer. Furthermore, we notice that the crystal structure near the interface becomes less dense as the solidification progresses, which implies a strong interaction between the crystal structure and convection. The change from fingers to plumes can be explained by a schematic diagram of Fig. 5. At the initial stages of solidification, fingers with a small wavelength appears on the mush–melt interface. After that, due to the dynamical behavior of fingers, finger merging occurs and the change in wavelength is observed, i.e., wavelength selection. Some of fingers becomes stronger rather than weaker and the upward flow remelts the crystals there. This is the onset of plumes or channel formation. The change from fingers to plumes is probably related to the structure of crystals. That is, plumes are likely to take place for a sparse structure rather than a dense one. The detail will be discussed in a future work.

Next, we examine the development of channels. Fig. 6 shows a sequence of photographs that illustrates the channel formation. A small channel is formed at a

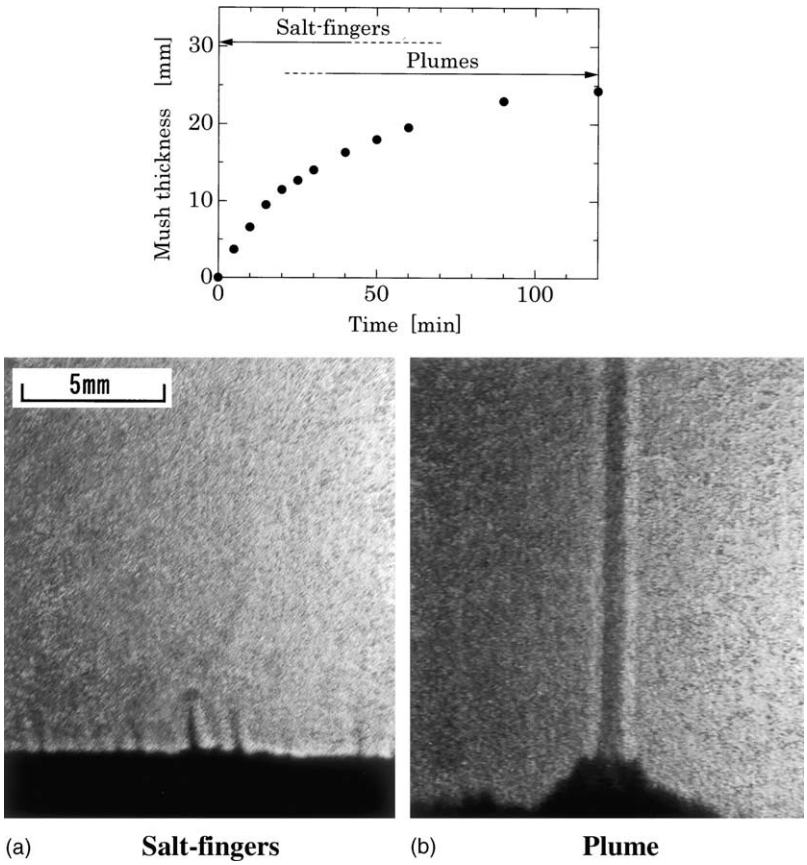

Fig. 3. Growth of mushy layer and shadowgraph images: (a) salt-finger convection, (b) plume convection.

localized region on the mush–melt interface due to remelting of crystals at the beginning. After that, the channel develops downward and, following the mush growth, the channel diameter gets larger. Also there is always a volcano-like buildup of crystals around the channel exit. The behavior of remelting is shown in Fig. 7. The roots of tertiary and secondary arms of dendritic crystals are remelted at first, and thus the dendritic crystals are broken into small ones. Tiny crystals are carried upward in the channel by plume convection, and larger chunks of crystals are dropped to the bottom. Qualitative explanation for the origin of channel formation is given as follows. The concentration in the mushy layer is unstably stratified and thermodynamic equilibrium is kept, as shown in the previous study [12]. As a result, there is a possibility that convection takes place within the mushy layer, but the onset of convection depends strongly on the mush structure, i.e., solid fraction or permeability. Once convection has started, the coupling between the convection and the mush structure becomes significant. The mush structure is determined by temperature, concentration and interstitial fluid velocity. In this system, remelting takes place in the region of upward flow, in the mushy layer, and thus the local solid fraction decreases there, leading to a reduction in the viscous resistance to the flow. Thus, a positive feedback mechanism strengthens the upward flow.

Next we describe the nature of plume convection ejected from the channel exit. Fig. 8 shows a sample photograph of this convection by a sequential three color light sheet method at $t = 60$ min. The flow direction is from red to blue line in each particle path during the exposure time, i.e., 5 s. Since downward flow exists around upward flow, the upward flow through the channel is not discernible. This observation is due to the following reasons. The plume has a three-dimensional structure, even in a Hele–Shaw cell, and the thickness of illumination is larger than the diameter of the channel. It is a surprise to us that the presence of downward flow has not been known previously and never been observed in the ordinary plumes due to thermal buoyancy. This may be attributed to the interaction of heat and mass transfer because of different diffusivities. Of particular interest here is the behavior of the downward flow near the channel exit, which leads to a buildup of crystals

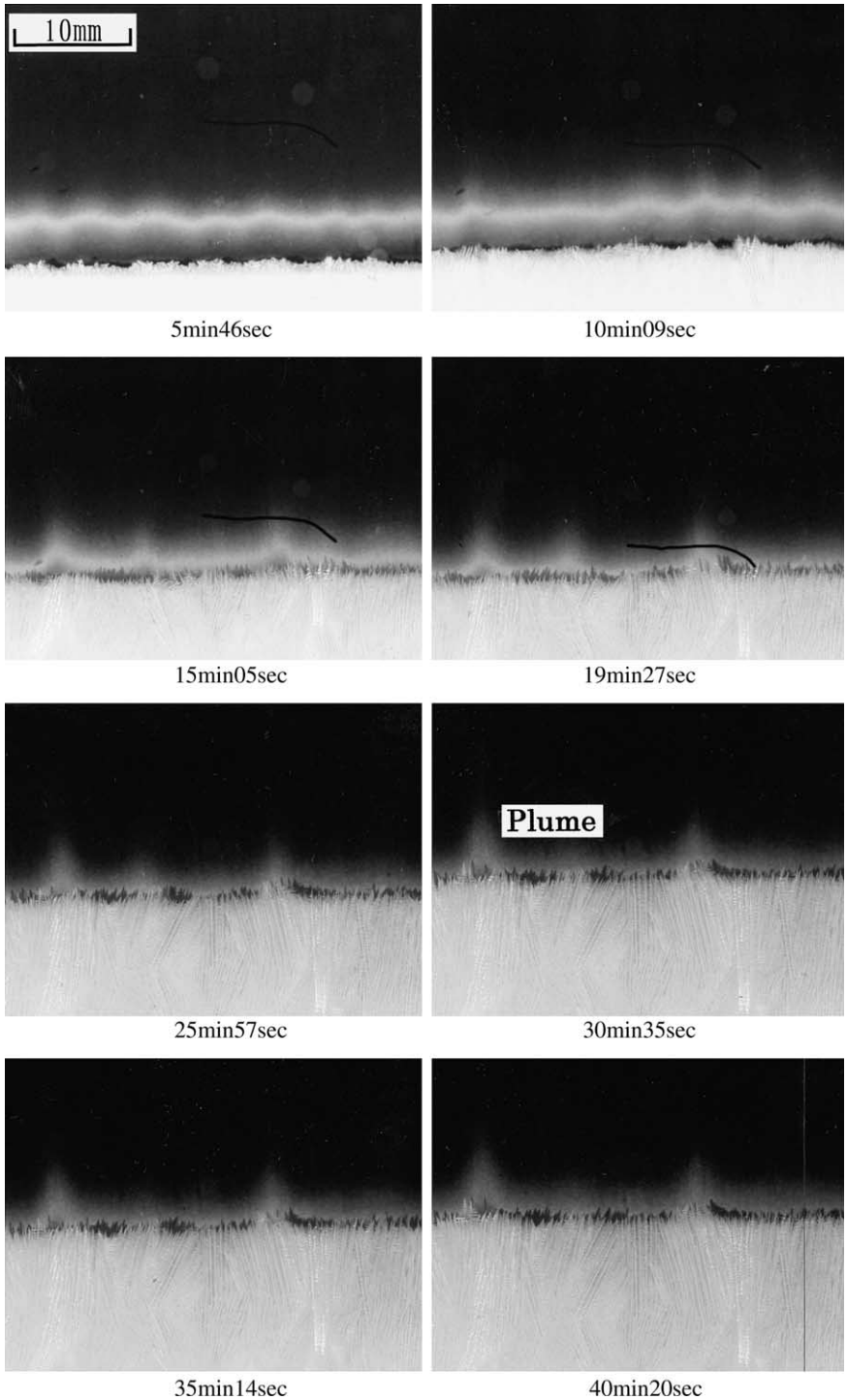

Fig. 4. Time history of isotherms visualized by a thermochromic liquid crystal sheet.

around the channel exit as shown in Fig. 6. Because a denser fluid is transported towards the channel exit by this downward flow, to be solidified there. There have been only two studies on three-dimensional numerical simulations of channel formation. Neilson and Incropera [13] solved the solidification process of an ammonium

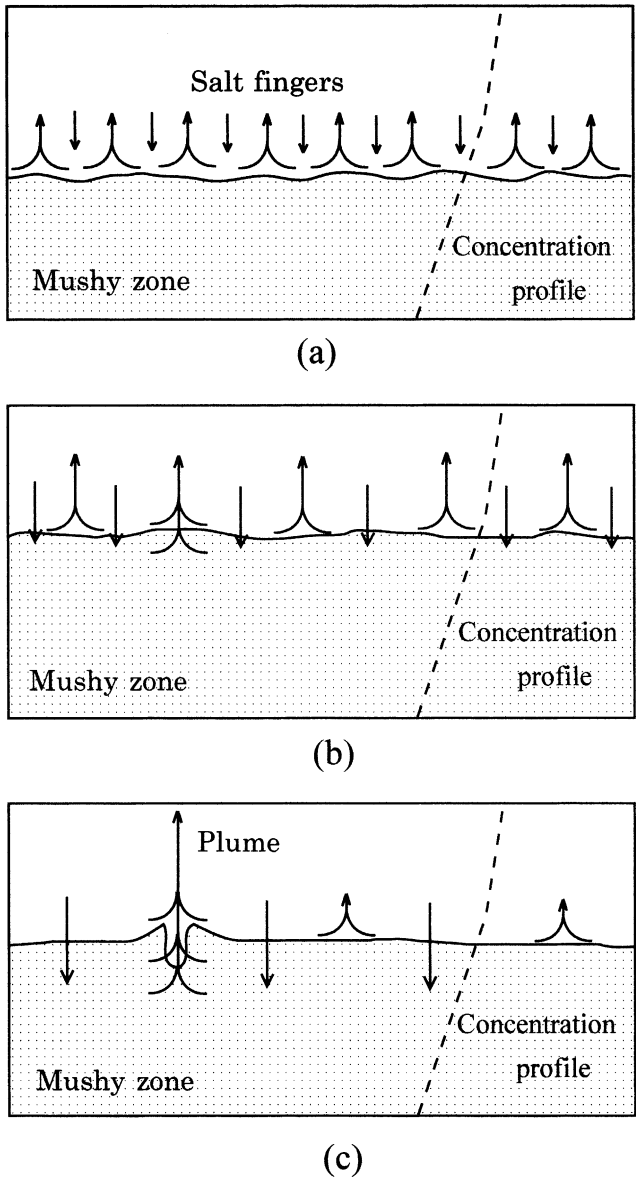

Fig. 5. Change from salt-fingers to plumes.

chloride solution in a cylindrical domain. Their results reproduced typical features of channels. However, by computing a rather large domain, the coarseness of the mesh and associated loss of resolution were not able to capture small-scale behavior, including salt-fingers and plumes. More recently Felicelli et al. [14] developed a three-dimensional finite element model and predicted a similar structure of plumes discovered in the present experiment for the solidification of superalloy based on Nickel. Thus it is believed that the plume structure discovered here is a general feature for multi-component solidification. Also the visualization photograph shows that part of the downward flow is observed over the mush–melt interface except in the channel region, which suggests the fluid motion in the musy layer.

Fig. 9 shows the upward velocity profile at the channel exit for $t = 60$ min., using a particle tracking velocimetry. The velocity is normalized by the maximum value, i.e., $u_{\max}$. The profile is quite different from that described by Poiseuille flow based on the channel diameter, which may be due to the permeability distribution across the channel. Time variation of the maximum velocity is shown in Fig. 10. The velocity increases slightly after the onset of plume and attains the maxi-

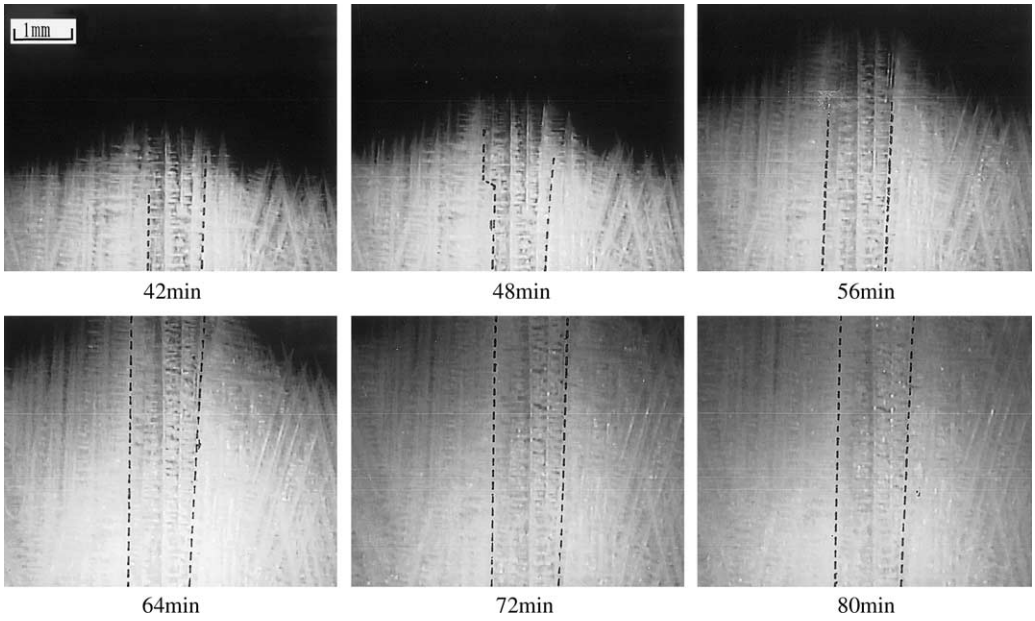

Fig. 6. Channel formation in the mushy layer.

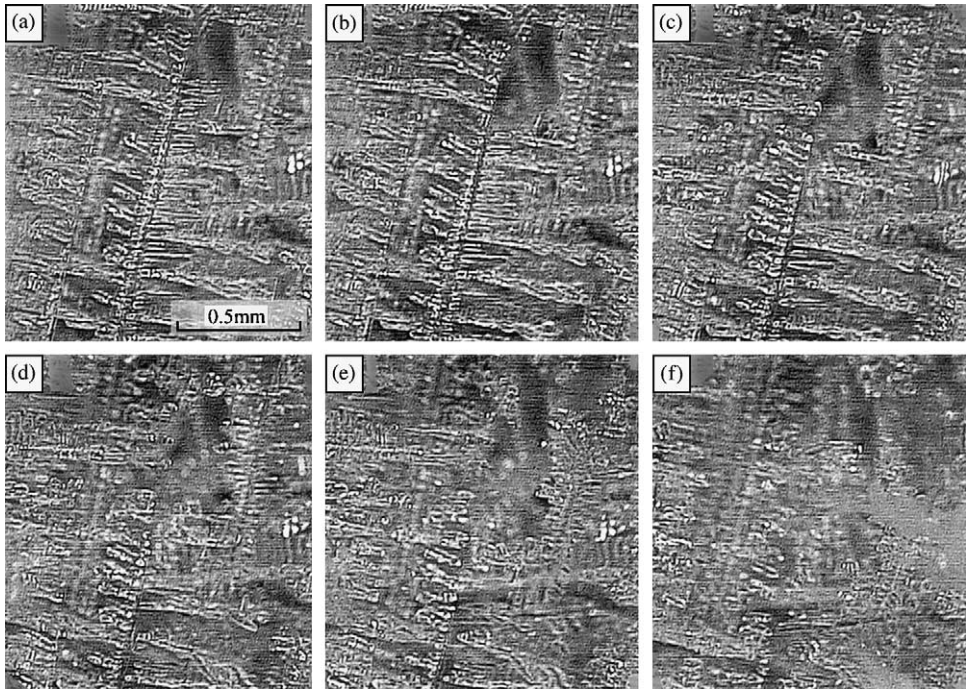

Fig. 7. Remelting of crystals in the mushy layer.

mum value of 3.8 mm/s at 80 min. This moment is close to the time in which the channel reaches the bottom of the cell. After that, the velocity gradually decreases.

Since the plume convection means the ejection of less denser fluid through the channel, the denser fluid near the mush–melt interface penetrates slowly through the

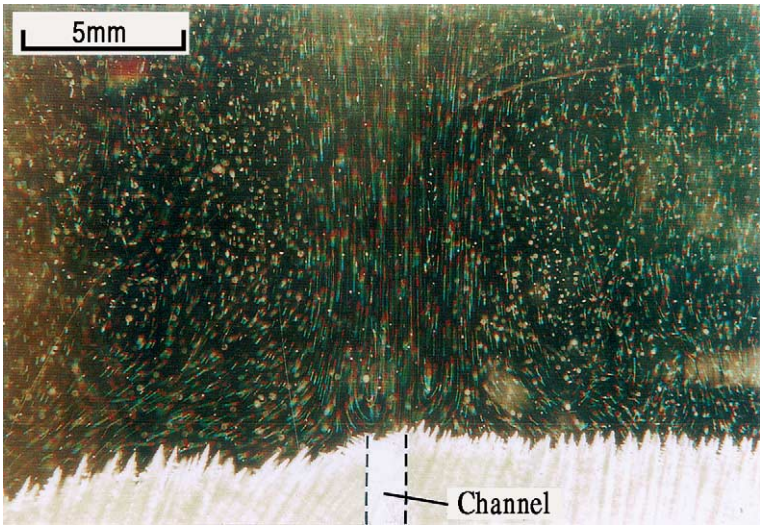

Fig. 8. Flow visualization of plume convection.

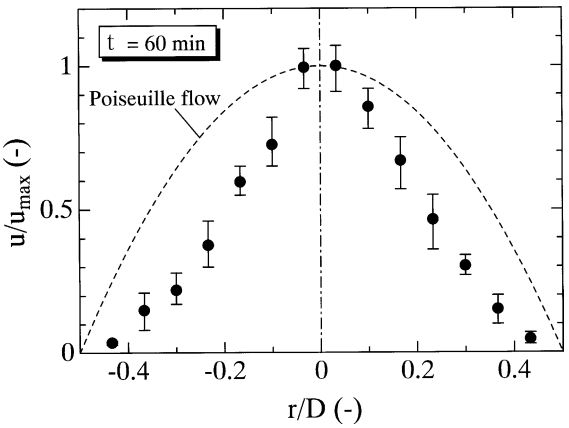

Fig. 9. Velocity profile in the plume at the channel exit.

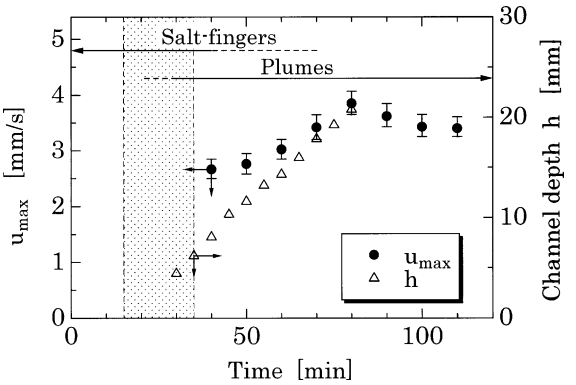

Fig. 10. Time variations of maximum velocity in the plume and channel depth.

larger part of the mushy layer. We estimate the interstitial velocity for downward flow from the mass balance. In this experiment, specifically at $t = 50$ min, the mass of less denser fluid is ejected from two plumes, with the channel diameter of 1.04 mm, the cross-sectional average velocity of 0.91 mm/s and the solid fraction of the mushy layer is 10% [12]. The estimated value of the downward flow is then 0.011 mm/s. In order to confirm this, we also measure the velocity using the dye tracing method. Fig. 11 shows a sequence of photographs that illustrate the dye movement. The dye trace moves downward almost uniformly in the space between the two channels. Quantitative data is obtained by recording the motion of the dye line using a time-lapse motion picture. Although the measured data depends on time, the velocity is 0.0087 mm/s during $t = 40$–60 min, which satisfactorily agrees with the predicted one.

4. Conclusions

We studied experimentally the structure of plumes generated during solidification of aqueous ammonium chloride solution. The velocities of plume convection in the melt layer and interstitial fluid flow within the mushy layer were measured. The following conclusive remarks were drawn.

1. The plume convection consists of the upward flow enveloped in the downward flow, i.e., double flow structure. The downward flow enhances the solidification in the neighborhood of the exit of channel emanating the plume.
2. Interstitial fluid within the mushy layer is observed to move downward uniformly, which is induced by the

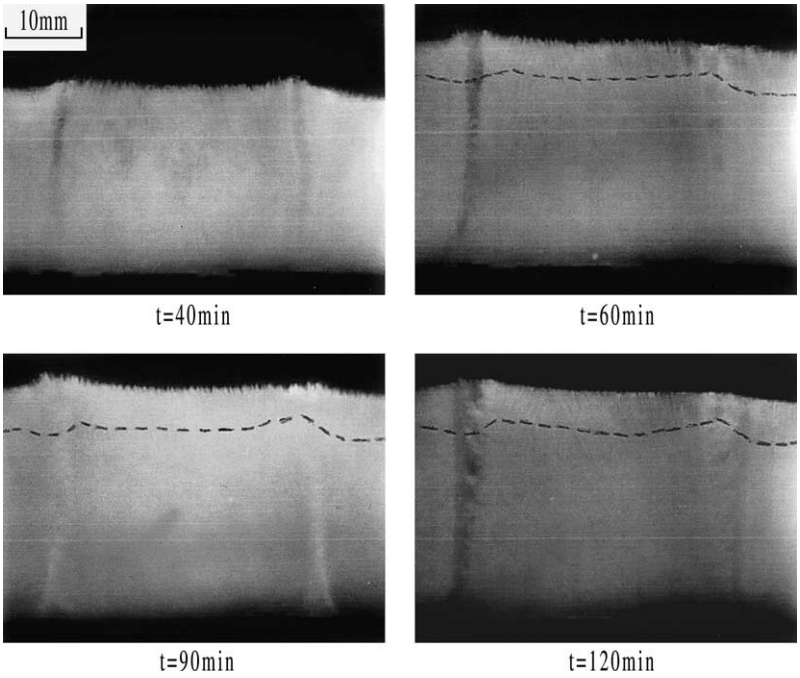

Fig. 11. Motion of a dye tracer in the mushy layer (- - - interface at $t = 40$ min).

plume convection. The measured velocity satisfactorily agrees with the predicted one.

The detailed mechanism of the onset of plumes is a subject of future work.

Acknowledgements

The present work was supported in part by a Grant-in-Aid for Science Research (no. 011650224) from the Ministry of Education, Culture, Sports, Science and Technology, Japan.

References

[1] R. Viskanta, Heat transfer during melting and solidification of metals, ASME J. Heat Transfer 110 (1988) 1205–1218.
[2] H.E. Huppert, The fluid mechanics of solidification, J. Fluid Mech. 211 (1990) 209–240.
[3] P.J. Prescott, F.P. Incropera, Convective heat and mass transfer in alloy solidification, Adv. Heat Transfer 28 (1996) 231–338.
[4] M.G. Worster, Convection in mushy layers, Annu. Rev. Fluid Mech. 29 (1997) 91–122.
[5] T. Nishimura, Transport processes during solidification of binary systems, Recent Res. Dev. Chem. Eng. 3 (1999) 237–257.
[6] C.F. Chen, F. Chen, Experimental study of directional solidification of aqueous ammonium chloride solution, J. Fluid Mech. 227 (1991) 567–586.
[7] C.F. Chen, Experimental study of convection in a mushy layer during directional solidification, J. Fluid Mech. 293 (1995) 81–98.
[8] S. Tait, C. Jaupart, Compositional convection in a reactive crystalline mush and melt differentiation, J. Geophys. Res. 97 (1992) 6735–6756.
[9] C.S. Magirl, F.P. Incropera, Flow and morphological conditions associated with unidirectional solidification of aqueous ammonium chloride, ASME J. Heat Transfer 115 (1993) 1036–1043.
[10] T.H. Solomon, R.R. Hartley, Measurements of the temperature field of mushy and liquid regions during solidification of aqueous ammonium chloride, J. Fluid Mech. 358 (1998) 87–106.
[11] T. Nishimura, M. Wakamatsu, Natural convection suppression and crystal growth during unidirectional solidification of a binary system, Heat Transfer Asian Res. 29 (2000) 120–131.
[12] T. Nishimura, K. Kotani, M. Ohtani, Concentration and temperature fields of mushy and melt regions during directional solidification of a binary system, ASME J. Heat Transfer, submitted for publication.
[13] D.G. Neilson, F.P. Incropera, Three-dimensional considerations of unidirectional solidification in a binary liquid, Numer. Heat Transfer, Part 1, 23 (1993) 1–20.
[14] S.D. Felicellie, D.R. Poirier, J.C. Heinrich, Modeling freckle formation in three dimensions during solidification of multicomponent alloys, Metall. Mater. Trans. B 29 (1998) 847–855.